Photocycle of Dried Acid Purple Form of Bacteriorhodopsin

Géza I. Groma, Lóránd Kelemen, Ágnes Kulcsár, Melinda Lakatos, and György Váró
Institute of Biophysics, Biological Research Center of the Hungarian Academy of Sciences, Szeged H-6701 Hungary

ABSTRACT The photocycle of dried bacteriorhodopsin, pretreated in a 0.3 M HCl solution, was studied. Some properties of this dried sample resemble that of the acid purple suspension: the retinal conformation is mostly all-*trans*, 15-*anti* form, the spectrum of the sample is blue-shifted by 5 nm to 560 nm, and it has a truncated photocycle. After photoexcitation, a K-like red-shifted intermediate appears, which decays to the ground state through several intermediates with spectra between the K and the ground state. There are no other bacteriorhodopsin-like intermediates (L, M, N, O) present in the photocycle. The K to K′ transition proceeds with an enthalpy decrease, whereas during all the following steps, the entropic energy of the system decreases. The electric response signal of the oriented sample has only negative components, which relaxes to zero. These suggest that the steps after intermediate K represent a relaxation process, during which the absorbed energy is dissipated and the protein returns to its original ground state. The initial charge separation on the retinal is followed by limited charge rearrangements in the protein, and later, all these relax. The decay times of the intermediates are strongly influenced by the humidity of the sample. Double-flash experiments proved that all the intermediates are directly driven back to the ground state. The study of the dried acid purple samples could help in understanding the fast primary processes of the protein function. It may also have importance in technical applications.

INTRODUCTION

Bacteriorhodopsin (BR), a light driven proton pump found in the cell membrane of *Halobacterium salinarum* was first isolated some 30 years ago (Blaurock and Stoeckenius, 1971). The studies concentrating on the structure and function of this protein revealed many details, beginning with the light absorption mechanism of the retinal bound to a lysine, to the final steps of proton translocation across the membrane (Lozier et al., 1975; Ebrey, 1993; Lanyi and Váró, 1995; Lanyi 2000). Dark adaptation of the protein preparation leads to a thermal equilibrium with the retinal in two different conformations: 40% all-*trans*, 15-*anti*, and 60% 13-*cis*, 15-*syn* form. Upon prolonged illumination the 13-*cis* retinal isomerizes to all-*trans*, forming the light-adapted BR (Konishi and Packer, 1976; Scherrer et al., 1987).

After light excitation, BR undergoes a photocycle with several spectrally different intermediates (K, L, M, N, O) (Lozier et al., 1975; Gergely et al., 1997). The intermediates have complex kinetic properties (Váró and Lanyi, 1990; Lozier et al., 1992; Ludmann et al., 1998b) outlined in different models. Between pH 4 and 9, the function of the BR can be described with a model containing reversible reactions in a single photocycle (Váró and Lanyi, 1990; Ames and Mathies, 1990; Lozier et al., 1992; Ludmann et al., 1998b). At ~pH 9.5, which is the pK_a of the proton release complex, BR exists in two states with presumable protonated and deprotonated glutamic acid (Balashov et al., 1996; Richter et al., 1996). In this pH region, the possibility of the two parallel photocycles is reasonable.

Crystallographic studies resulted at 1.55 Å resolution structure of the protein (Subramaniam, 1999; Luecke et al., 1999b).The structure of several photocycle intermediates have also been resolved (Edman et al., 1999; Luecke et al., 1999a; Vonck, 2000; Sass et al., 2000).

When pH is changed from neutral to acidic, several spectrally different species appear (Mowery et al., 1979; Váró, and Lanyi, 1989; De Groot et al., 1990). At pH below 2, the proton acceptor Asp^{85} is protonated, which leads to different photocycles depending on the ion content of the bathing solution (Váró and Lanyi, 1989; Tokaji et al., 1997). When the solution contains sulfate but no chloride ions, the photocycle of the "acid blue BR" has a K-like and an L-like intermediate (Váró and Lanyi, 1989). In the presence of chloride ions, the photocycle of the "acid purple BR" contains mostly red-shifted intermediates. Compared with BR, the decay of the excited state to a K-like intermediate is slower in this case (Logunov et al., 1996). After a K-like intermediate, an O-like one was observed (Váró and Lanyi, 1989). Later, it was shown that the photocycle also has an N-like intermediate (Tokaji et al., 1997). Fourier transform (FT) Raman studies revealed that the acid purple BR contains mostly all-*trans* retinal (Kelemen et al., 1999). The photocycle of acid purple BR was compared with that of halorhodopsin, using time-resolved Fourier transform infrared (FTIR) spectroscopy (Mitrovich et al., 1995)

Water has an important role in the function of BR, as was revealed by studies on dehydrated samples. During light-adaptation, the 13-*cis* to all-*trans* transition of the retinal is increasingly hindered with decreasing humidity; at ambient humidity ($P/P_o = 0.5$) it is almost totally abolished (Korenstein and Hess, 1977a; Váró and Keszthelyi, 1983). The

Received for publication 16 January 2001 and in final form 22 August 2001.

Address reprint requests to Dr. György Váró, Institute of Biophysics, Biological Research Center of the Hungarian Academy of Sciences, Szeged, Temesvari KRT 62, H-6701 Hungary. Tel.: 36-62-432232; Fax: 36-62-433133; E-mail: varo@nucleus.szbk.u-szeged.hu.

0006-3495/01/12/3432/10 $2.00

photocycle of the dried sample stops at intermediate M and no proton transport occurs (Korenstein and Hess, 1977b; Váró and Keszthelyi, 1983). The dehydration of the sample hinders the conformational change of the protein (Váró and Eisenstein, 1987). The photocycle terminates at intermediate M_1, with the protein still in the extracellular conformation (Betancourt and Glaeser, 2000; Dencher et al., 2000), and returns back to ground-state BR after a multiexponential decay (Ganea et al., 1997). The kinetics of the photocycle are strongly dependent on the water content of the sample (Korenstein and Hess, 1977b; Váró and Keszthelyi, 1983; Ganea et al., 1997). FTIR studies revealed the importance of the bound water in the structure and function of BR (Maeda et al., 2000).

On electrically anisotropic samples containing oriented BR molecules, photoelectric response signals could be measured (Bamberg et al., 1981; Keszthelyi and Ormos, 1983; Dér et al., 1985). In the pH range of 4 to 9, the electrogenicity of the intermediates was determined, which provided information about the proton translocation steps of the photocycle (Ludmann et al., 1998a; Dér et al., 1999). When the pH was set below 1 with HCl, electric signal measured during a continuous illumination of the sample proved that the acid purple BR transports chloride ion across the membrane (Dér et al., 1991). Despite some controversial results (Moltke and Heyn, 1995), the careful study of the transient photovoltage response of the acid purple BR confirmed this conclusion (Kalaidzidis and Kaulen, 1997).

The effect of water on the electrogenic steps of the photocycle was investigated by the use of purple membranes deposited electrophoretically on a conducting glass and air-dried. The analysis of the electric signals, measured on dried oriented samples, revealed that the charge moves inside the membrane, but no net charge translocation occurs (Váró and Keszthelyi, 1983, 1985).

In wild-type BR, the excitation of intermediate M produces another photocycle, with a shortcut back to the ground state (Litvin and Balashov, 1977; Ludmann et al., 1999). Intermediate N was also proven to be photoactive (Kouyama et al., 1988; Váró and Lanyi, 1990). The excitation of intermediate K drives the photocycle directly back to the ground state (Ormos et al., 1983; Groma et al., 1995).

In this study, our purpose was to get information about the early, red-shifted K and K-like intermediates which appear in the BR photocycles. The properties of the dried sample prepared with HCl having a pH <1 are investigated. Its photocycle has only red-shifted K-like intermediates, which appear rapidly, and their decay is multiphasic in the ms time domain. The absorption kinetic signals were fitted with different photocycle models containing several K-like intermediates with slightly different spectra. This photocycle is compared with the other red-shifted intermediates as those appearing in the photocycle of the 13-*cis* and vacuum-dried BR.

The knowledge of the kinetic properties of dried acid purple BR (APB) is important both for basic research and application. As the properties of the K-like intermediate are changed, the use of these samples could help in the future in understanding the properties of the excited states of BR. Also, having a simple, two-state photocycle, it could be used as a data storage material.

MATERIALS AND METHODS

Purple membrane suspension was obtained by the standard procedure from *Halobacterium salinarum* strain S9 (Oesterhelt and Stoeckenius, 1974). For absorption kinetic measurements the samples were prepared by drying 0.5 ml suspension on a 5 cm^2 glass. The suspension contained 16 μM purple membranes and 3% wt/vol gelatin (Sigma, St. Louis, MO) (Batori-Tartsi et al., 1999). Electric signal measurements were performed on dried oriented samples prepared by electrophoretic deposition of the purple membranes on an indium-tin-oxide–conducting glass connected as the anode in the electric circuit (Váró and Keszthelyi, 1983). To obtain the APB sample, the dried sample was soaked 3 min in water, then transferred for 1 min to 0.3 M HCl (pH ~0.5) and air-dried.

During the measurements, the sample was kept in a temperature- and humidity-controlled holder. To equilibrate the water content of the purple membranes at the desired relative humidity, the sample was kept overnight in the sample holder over various saturated salt solutions (Weast, 1971). The measuring conditions were 20°C and 51% relative humidity obtained over saturated solution of $Ca(NO_3)_2$, unless otherwise indicated.

The absolute spectrum of the sample was measured with a Unicam spectrometer (UV 4). FT Raman spectra were measured in a Bruker FRA 106 spectrometer equipped with a Nd:YAG laser, by averaging 1000 scans.

The samples were excited by a frequency-doubled Nd:YAG laser (Continuum, Santa Clara, CA, Surelite 10, $\lambda = 532$ nm). Time-resolved spectroscopy with gated optical multichannel analyzer provided difference spectra at various time points of the photocycle (Zimányi and Lanyi, 1989). The difference spectra were analyzed by singular value decomposition (SVD) (Golub and Kahan, 1992). This mathematical analysis provided the minimum number of components present in the set of spectra. It was possible to determine the spectral component bearing not only noise. The

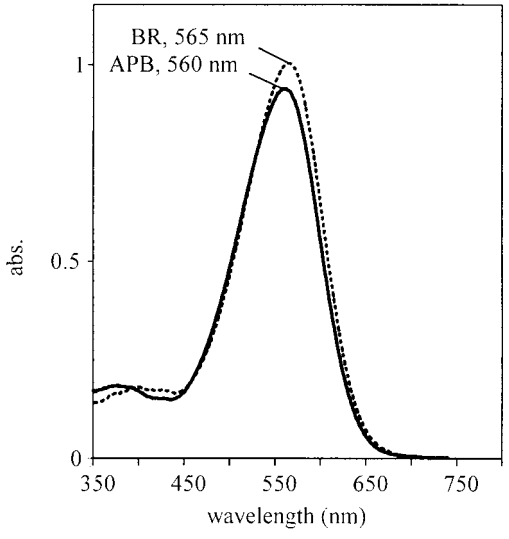

FIGURE 1 The spectrum of dried BR and APB. Measuring conditions: 20°C and 51% relative humidity.

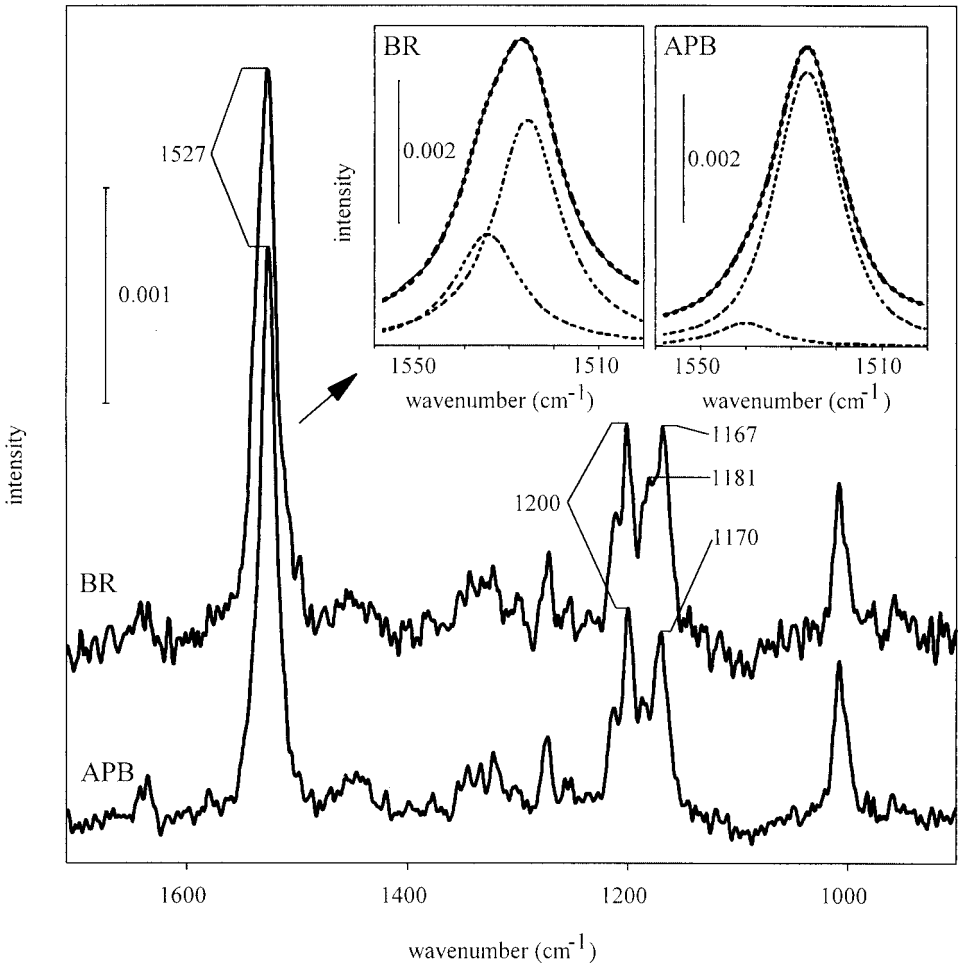

FIGURE 2 FT Raman spectra of dried BR and APB. The insets show the decomposition of the main peak with two Lorentzians, corresponding to all-*trans* (1526 cm^{-1}) and 13-*cis* (1535–1540 cm^{-1}) retinal.

reconstructed noise filtered difference spectra were used to calculate the spectra of photocycle intermediates (Gergely et al., 1997; Kulcsár et al., 2000).

Time-dependent absorption kinetic signals were measured at five wavelengths (410, 500, 560, 610, and 670 nm) in a time interval from 500 ns to 1 s, using a transient recorder card (NI-DAQ PCI-5102 National Instruments, Austin, TX) with 16 MB memory. The data sampled with 50 ns dwell time were converted to a logarithmic time scale by averaging on logarithmically equidistant intervals. Each measurement was the average of 100 signals. Model fit was performed with the RATE program to obtain microscopic kinetic parameters (Ludmann et al., 1998b). The energy diagram of the reactions was calculated from the temperature dependence of the rate constants using the Eyring program (Ludmann et al., 1998b).

Light-induced electric response signals were measured on the set-up described earlier (Gergely et al., 1993). The time resolution of the measuring circuit for both the absorption kinetic and electric signal measurements was 100 ns. The electrogenicity of an intermediate was defined as the change in the electric dipole moment of the protein found in that intermediate, relative to its ground state (Trissl, 1990; Gergely et al., 1993). The relative electrogenicity of the intermediates were calculated from the measured electric signal using the earlier determined kinetic parameters (Gergely et al., 1993; Ludmann et al., 1998a).

Double-flash experiments were carried out with the use of a nitrogen laser-driven dye laser (sulforhodamine B, $\lambda = 610$ nm), synchronized with variable retardation to the Nd:YAG laser.

RESULTS

The spectrum of BR shifts with 5 nm toward blue after the acid treatment described in Materials and Methods (Fig. 1). The shift is accompanied by a small amplitude decrease. In dried samples the process of light adaptation is hindered. FT Raman measurements helped to clarify the 13-*cis* to all-*trans* ratio in the sample (Fig. 2). The spectrum of BR in the fingerprint region, contained an extra peak at 1167 cm^{-1}, in addition to the peaks at 1181 and 1200 cm^{-1} (Smith and Mathies, 1985). The fingerprint region of the APB was similar to that corresponding to the light-adapted BR published earlier, having peaks at 1170 and 1200 cm^{-1} (Smith and Mathies, 1985). We decided to look more carefully at the broad peaks corresponding to C═C stretching, charac-

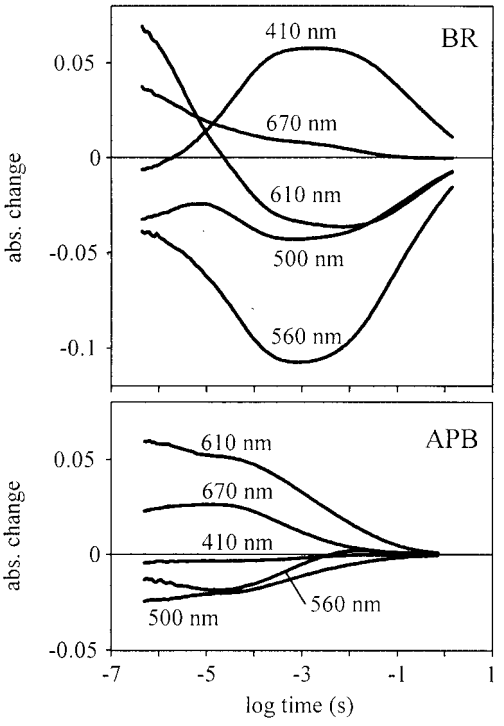

FIGURE 3 Absorption kinetics measured on dried BR and APB. Measuring conditions were the same as in Fig. 1.

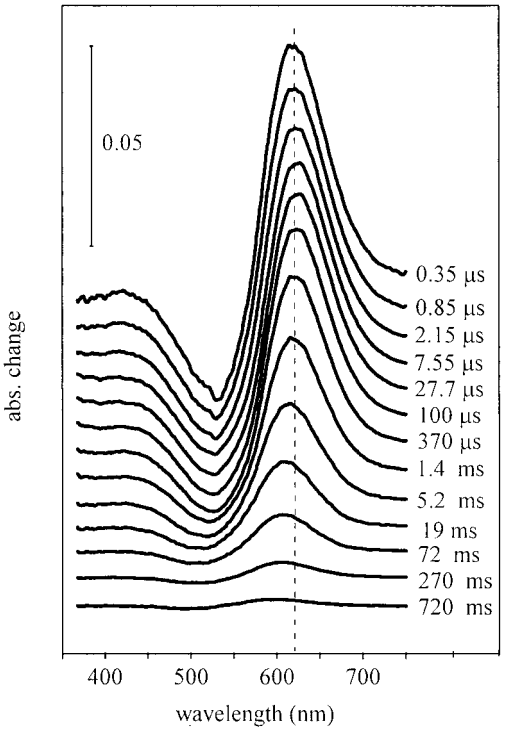

FIGURE 4 SVD-filtered difference spectra measured on APB at the indicated time after the photoexcitation. Measuring conditions were the same as in Fig. 1.

teristic to the isomer composition of the retinal at 1527 cm^{-1}. The peak corresponding to BR had a 22 cm^{-1} width at half maximum, showing that it is a mixture of 13-*cis* and all-*trans* chromophore. That corresponding to APB had a width of 15 cm^{-1} corresponding almost totally to all-*trans* chromophore (Smith and Mathies, 1985). For a better mathematical characterization, the peaks were fitted with Lorentzians. Both the BR and APB could be fitted with two components, where the peak corresponding to the all-*trans* retinal at 1526 cm^{-1} increased in APB, whereas that corresponding to 13-*cis* retinal $\sim$1536 cm^{-1} decreased (Fig. 2, *insets*). This second peak is shifted to 1540 cm^{-1} in APB, but its amplitude is so small that the error of the fit makes the position of the peak uncertain. These demonstrated that the APB sample contains almost homogeneously all-*trans* retinal.

Although acid treatment caused only slight changes in the absorption spectrum of the ground state, dramatic changes occurred in the absorption kinetic signals. After laser excitation, the dried BR shows a characteristic absorption change at 410 nm, corresponding to the appearance and disappearance of intermediate M (Fig. 3). When APB was photoexcited, no change characteristic for intermediate M at 410 nm could be observed. In the red region a very fast absorption increase occurred, whereas at the main peak (560 nm) or at lower wavelengths, the absorption decreased. The rise of the absorption kinetic signals was faster than the time resolution of the measuring system, whereas the decay was multiphasic in the ms time domain.

To investigate the photocycle of the APB, the spectra of intermediates were determined from transient difference spectra, measured with an optical multichannel analyzer. The SVD analysis of the difference spectra resulted in the existence of four components which contained not only noise, but had the characteristic of a difference spectrum. These components had weight factors between 140 and 1.6; all the others were below 0.7. The autocorrelation calculated for both the spectra and amplitude of the first four components were >0.86; the other autocorrelation factors were <0.5. The reconstruction of the difference spectra with these significant components provided a set of noise-filtered difference spectra (Fig. 4). All difference spectra show a maximum at 620 nm, which corresponds to the appearance of a red-shifted intermediate. With increasing time, this maximum decreases and shifts slightly toward blue, which implies that more than one intermediate is formed during the photocycle. The existence of the four components in the SVD analysis suggested the existence of four spectrally different intermediates during the photocycle. The spectra of the intermediates were calculated as described earlier (Gergely et al., 1997).

An important parameter in the calculation of the spectra is the percentage of the photoconversion of the sample. This

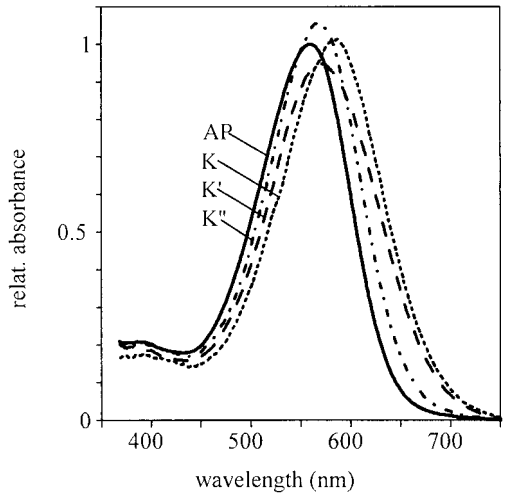

FIGURE 5 The spectra of intermediates calculated from the difference spectra shown in Fig. 4.

was determined in two ways, resulting in the same value. First, a dried BR sample was excited, using the assumption that the quantum efficiency of the sample did not change when it was acid-treated. In this case, we could calculate the percentage of photoconversion (Ganea et al., 1997). The second value was derived during the fitting procedure, when the basic requirements of the intermediate spectra were considered: nonnegative absorption, single peak, shapes which resemble the predicted skewed spectrum of a rhodopsin-type pigment. The calculation resulted in three spectrally different intermediates (K, K′, K″) with absorption maxima between 570 and 590 nm (Fig. 5) and another intermediate (AP′) with a similar spectrum to that of the ground state (AP). The first intermediate spectrum had the largest shift, with an absorption maximum at 587 nm. As the photocycle proceeds, this shift decreases to 573 nm for the K′ and 570 nm for K″.

Three models were fitted to the absorption kinetic data

A) Three parallel photocycles, each containing one K-like and one AP′ intermediate. This model could not fit the early part of the photocycle. The decreasing absorption change at 500 and 610 nm is accompanied by an increasing absorption change at 560 and 670 nm (Fig. 6 *A*), which can not be described by a continuous decrease in concentration of red-shifted intermediates. Instead, it reveals a transition between two slightly different red-shifted intermediates, contradicting this model.

B) Parallel photocycle branched at intermediate K.

$$K \Leftrightarrow K' \Leftrightarrow AP' \Rightarrow AP \quad \text{and} \quad K \Leftrightarrow K'' \Leftrightarrow AP' \Rightarrow AP$$

and

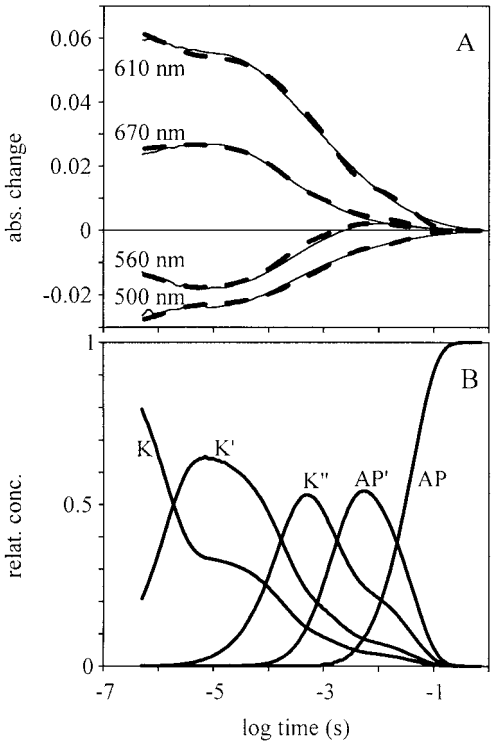

FIGURE 6 (*A*) The fit of the sequential photocycle model (*dashed lines*) to the time-dependent absorption kinetic signals (*continuous lines*). (*B*) Time evolution of the concentration of intermediates. The error of the fit was ±3%.

C) Sequential model:

$$K \Leftrightarrow K' \Leftrightarrow K'' \Leftrightarrow AP' \Rightarrow AP$$

In models B and C, all reactions were considered reversible, except the last one, which ensured the unidirectionality of the photocycle. The fitting procedure left all the reactions reversible. The parallel model contains 11 independent fitting parameters, whereas the sequential one contains only eight. Both models gave similar goodness of fit and similar time-dependent concentration change of intermediates. In Fig. 6 the fit and the concentration change of intermediates is shown for the sequential model.

To decide which model is valid and determine the energetic scheme of the photocycle, the temperature dependence of the absorption kinetic signals was measured between 5 and 30°C (not shown). The Eyring plot (ln k vs. $1/T$, where k is the rate constant of the transition and T is the temperature measured in K) of all the rate constants were linear only for the sequential model (not shown). In the case of the parallel model, several Eyring plots were curved. The activation free energy, enthalpy, and entropy of the photocycle transitions were calculated as previously (Ludmann et al., 1998b; Kulcsár et al., 2000). In the case of the parallel photocycle, several activation enthalpies were negative, which have no physical meaning. Based on these facts, the

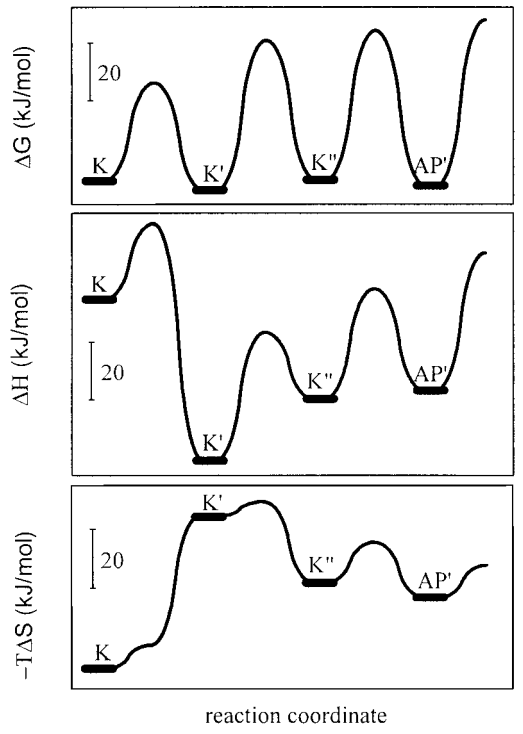

FIGURE 7 The free energy, enthalpy, and entropic energy diagram of the APB calculated from the Eyring plots of the temperature-dependent absorption kinetic signals.

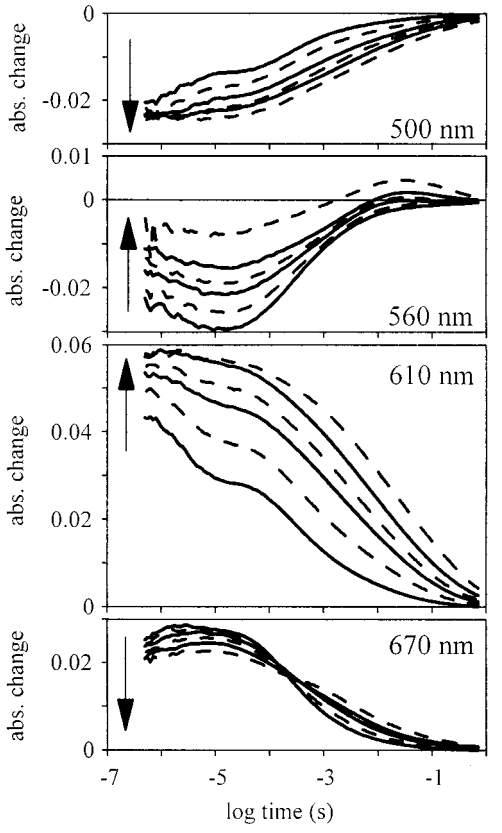

FIGURE 8 Time-dependent absorption kinetic signals measured on APB at different humidities. The arrows show the direction of the decreasing relative humidity: 65, 51, 43, 33, 22, and 12%.

sequential model was accepted. As the reactions were reversible, from the activation parameters the relative free energy, entropy, and enthalpic energy levels of the intermediates were calculated and plotted against the reaction coordinate (Fig. 7).

By decreasing the relative humidity from 65 to 12% in the sample holder, the decay time of the photocycle increases with almost one order of magnitude (Fig. 8). The fast phase in the decay of intermediate K in the μs time domain, observed at 610 nm, disappears. At 560 nm a positive feature appears in the 100 ms time domain, which can be attributed to the increase of the concentration of intermediate K$''$.

The double-flash experiment provided information about the absorption kinetic signal corresponding to the excitation of the photocycle intermediates measured at 610 nm (Fig. 9 *A*). From the absorption kinetic corresponding only to the Nd:YAG laser, it was estimated that ~30% of the APB was excited. From the double flash signal, the signal corresponding to that measured with only the Nd:YAG laser and 70% of the signal measured with only the dye laser were subtracted. The remaining signal is produced by the excitation of the intermediates present in the sample at the moment of the second flash. This procedure was repeated for three delay times: 1.7, 12, and 740 μs, when mostly K, K$'$, and K$''$ intermediates were present, respectively (Fig. 9 *B*). The same double-flash measurements were repeated, monitoring the sample at 500 nm, with similar results (not shown).

Electric signal measurements on BR had both negative and positive components. In APB the positive component disappears, and the negative component shows multiphasic decay, similar to that observed in the absorption kinetic signals (Fig. 10). In contrast to the BR form, the negative component reaches its minimum at 10 μs. The measured voltage signal show the real charge motions up to several ms, denoted by a dashed line on Fig. 10, because the time constant (RC) of the measuring circuit was ~30 ms. The relative electrogenicities of the intermediates were calculated by using the time-dependent concentrations of the intermediates and the measured electric signals up to 8 ms. Taking the electrogenicity of K = −1 the calculation gave the electrogenicity of K$'$ = −1.3, K$''$ = −0.45, and AP$'$ = 0.41. It should be mentioned that the calculated electrogenicity of AP$'$ could already be influenced by the RC of the measuring circuit.

DISCUSSION

The study of APB samples reveal interesting features of the transport mechanism of the protein. Whereas the spectrum

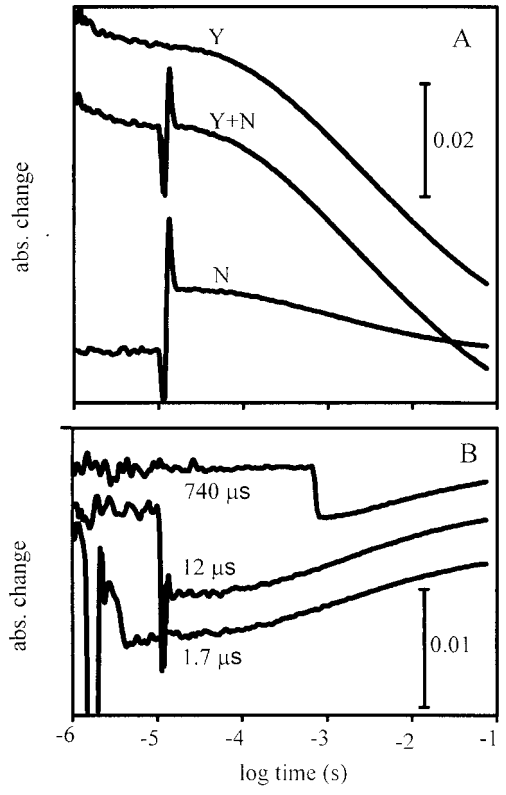

FIGURE 9 (*A*) Absorption kinetic signals measured at 610 nm in a double excitation experiment: (Y) the signal measured, when only the Nd:YAG laser was fired; (N) the signal measured when only the dye laser was fired; and (Y+N) the signal measured after the double flash, when the dye laser is retarded with 12 μs. (*B*) The resultant signal corresponding to the excitation of the intermediates present at three different time delays after the photoexcitation.

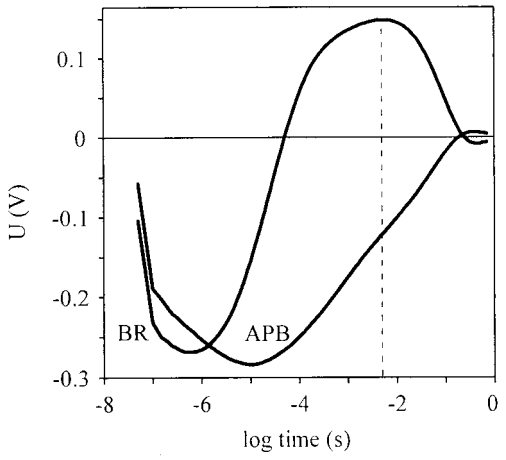

FIGURE 10 Photoelectric signals measured on dried oriented BR and oriented APB. Measuring conditions were the same as in Fig. 1.

is only slightly shifted toward blue, in comparison with BR (Fig. 1), the photocycle is very different. FT Raman measurements pointed out the change in the retinal isomer composition (Fig. 2) from a mixture of all-*trans* and 13-*cis* in BR to an almost total all-*trans* content in APB. From this change it was expected that the spectrum would shift toward red, because the all-*trans* retinal in the protein has its absorption maximum at 568 nm and that corresponding to 13-*cis* retinal at 548 nm (Konishi and Packer, 1976; Pettei et al., 1977). The shift to an almost total all-*trans* retinal content, during acid treatment, assures an almost homogeneous sample. In lowering the pH with HCl, the acid purple form of BR appears (Fischer and Oesterhelt, 1979). The Asp^{85} is titrated (Metz et al., 1992; Balashov et al., 1995), and chloride ions are bound to the protein (Váró and Lanyi, 1989). The small spectral shift toward blue (Fig. 1) indicates that although the net charge of the protein is preserved, the electric field around the retinal is changed. The several percent decrease in spectral amplitude could be attributed to either a change in the extinction coefficient or a partial denaturation of the protein during the acid treatment. This second possibility is supported by the absorption increase ~370 nm (Fig. 1), indicating the appearance of a small amount of free retinal in the sample.

From the absorption changes (Fig. 3) it can be noticed that although BR has a complex photocycle, in the case of APB the photocycle is much simpler. The photocycle of APB has no M-like intermediate with a deprotonated Schiff-base, because the acceptor Asp^{85} is already protonated from the exterior. In acid purple BR suspension, in addition to the red-shifted K-like intermediate, slightly blue-shifted L- and N-like intermediates appear (Váró and Lanyi, 1989; Tokaji et al., 1997). In APB only red-shifted intermediates could be identified (Fig. 5). All the absorption changes show a fast, unresolved rise and multiphasic decay, except that measured at 560 nm. At this wavelength, a small maximum in the ms time domain was observed, which could be attributed to the increased extinction of the intermediate K″ (Fig. 5).

Time-resolved difference spectra (Fig. 4) having one absorption maximum at ~600 nm suggest a simple photocycle. The mathematical analysis revealed that not one but at least three, spectrally slightly different intermediates are required to describe the spectral changes (Fig. 5). The existence of several K-like intermediates in sequence or in parallel was already discussed earlier by using low temperature spectroscopy (Shichida et al., 1983; Balashov et al., 1991) or FTIR spectroscopy (Sasaki et al., 1995b; Dioumaev and Braiman, 1997). Based on the analysis of the absorption kinetic signals it was necessary to introduce another intermediate AP′, which is spectrally identical to AP. The same procedure was followed as in the case of the chloride ion pumping pharaonis halorhodopsin, where an intermediate with similar spectrum to that of the ground state protein was introduced in the photocycle (Váró et al., 1995; Kulcsár et al., 2000). Although the protein is already in its ground-state conformation, the absorbed light energy is not yet totally dissipated. The protein is in an energized

state in equilibrium with the previous intermediates. As the energy is dissipated, the ground state is reached. The spectral shift of the consecutive K-like intermediates toward the spectrum of AP also suggests that the absorbed light energy stored in the retinal pocket is transferred to the protein and is dissipated.

Independently from the fitted parallel or sequential model, the change of concentration of intermediates was the same in both cases. The appearance of the intermediates was separated in time by at least one order of magnitude. The next intermediate appears when the previous already decreases, suggesting a sequential appearance of them. (Fig. 6). In the case of the parallel model, the time constants belonging to the appearance and decay of intermediate K′ assured its accumulation in the μs time domain, but its decay was mainly through the K″ branch. The back reaction K′ to K was more than one order of magnitude faster, compared with the decay time of K′ to AP′. The energetic calculations based on the temperature dependence of the absorption kinetic signals proved the validity of the sequential model. Only this model gave a set of parameters which had physical meaning, and an energetic scheme of the photocycle could be drawn (Fig. 7).

The free energies of the intermediates are at almost the same level, leading to a minimum energy requirement for the photocycle. The last step, the AP′ to AP transition is the only unidirectional one, which assures the unidirectionality of the whole photocycle. During the K to K′ transition, an enthalpy decrease and entropic energy increase (entropy decrease) happens, which is equivalent to an increase in the order of the protein conformation. This could be the energy transfer step from the retinal to the protein, accomplished by small changes in the position of the amino acid side chains. As there is no charge transfer across the membrane, this entropy change is dissipated in the further steps of the photocycle.

The removal of the tightly bound water from the extracellular half-channel slows down the photocycle (Fig. 8) (Váró and Keszthelyi, 1983). The back reactions become dominant at the beginning of the photocycle. This suggests that the slight conformational changes producing the increased entropy become even smaller, and the protein motions are more and more hindered. The increase of the maximum in the absorption kinetic signal measured at 560 nm shows that K″, which has the smallest entropic energy, accumulates in greater amounts.

The absorption kinetic signals of the intermediates, measured at 610 nm with double-flash excitation (Fig. 9 *B*), show a decrease corresponding to a disappearance of the absorbing intermediate. The same signals measured at 500 nm (not shown) exhibit an absorption increase with the same kinetics, which corresponds to a reappearance of the AP. The decay of the difference signal after the second flash is similar to that of the photocycle. It does not contain another kinetic component. These signals were measured at two wavelengths and three different delay times, corresponding to the maximum concentration of the three consecutive K-like intermediates, and they were similar. No other type of absorption change that would reveal the existence of another intermediate state could be observed. The excitation of all K-like intermediates produces a rapid depletion of the intermediates and increase in the AP concentration, meaning that the protein most likely returns directly to its ground state. The similarity in the decay of the double-flash signals suggests that the structural differences of the three K-like intermediates are minor, which does not affect their properties of direct photoconversion back to APB.

The measured charge motions (Fig. 10) support the energetic scheme. In BR, the negative electrogenicity of the K and L intermediates results from a negative voltage after the photoexcitation, which become positive as intermediate M accumulate. In the case of APB, the negative signal increased to 10 μs, when intermediate K′ reached its maximum concentration. Similar signal was observed on BR incorporated into a lecithin-impregnated collodion film at low pH (Drachev et al., 1981). The initial charge separation in K was followed by some charge rearrangements in the protein, yielding a voltage increase. The further charge motions resulted a decrease in the measured voltage, both for K″ and AP′. The last step was not resolved because of the discharge with the RC of the measuring system. Because of the fact that there is no net charge transfer across the membrane, it can be concluded that during this step all the charges reach their ground-state position.

All photocycles of retinal proteins have a red-shifted, K-like intermediate appearing in the ps time scale. In the case of BR, three requirements are essential to proceed with the proton-pumping photocycle: the proton acceptor Asp^{85}, a proton wire from the acceptor to the proton release group, and the possibility of conformational change. The photocycle passes from intermediate K to L by a conformational rearrangement around the retinal. The next transition is the deprotonation of the Schiff base, resulting in the blue-shifted M intermediate.

When BR is moderately dehydrated, the possibility of the conformational change resulted in a very low concentration of intermediate L (Ganea et al., 1997). The tightly bound water molecules in the extracellular half channel are still present. The photocycle stops at M, before the switch step, without pumping the proton through the membrane (Ganea et al., 1997). The steps, which need a conformational change, are hindered. As the photocycle in dried sample proceeds to intermediate M, it is not obvious from the fit that the conformational rearrangements during intermediate L are not present or this intermediate does not accumulate for kinetic reasons.

When the proton acceptor is removed by site-directed mutagenesis or titration (Butt et al., 1989; Balashov et al., 1996), the photocycle proceeds from intermediate L to N,

but neither intermediate M nor proton transport could be observed. Both the photocycle of BR at low pH and that of the mutant D85T pumps chloride ions through the membrane (Dér et al., 1991; Sasaki et al., 1995a). In the case of APB, the hydration hindrance blocks the conformational changes and the photocycle stops at intermediate K, followed by a slow process of dissipation of the absorbed energy.

Three photocycles are very similar: the 13-*cis* photocycle (Gergely et al., 1994), the vacuum-dried one, when the tightly bound water is removed (Kovács and Váró, 1988), and the photocycle of APB. In vacuum-dried and APB photocycle, the common features are the hindered conformational change of the protein and the missing connection between the Schiff base and proton acceptor. The role of the flexibility of the protein is pointed out by the humidity dependence of the AP photocycle. The similar photocycle of BR containing 13-*cis* retinal suggests the possibility that, in this case, the changed retinal conformation breaks the H bond toward Asp^{85} and the protein around the retinal becomes more rigid. The absorbed energy is slowly dissipated through the protein.

It was shown earlier that the lifetime of the excited state increases almost with one order of magnitude in the acid purple BR (Logunov et al., 1996). The high protein density of the APB samples and the anisotropy of the oriented APB samples make them very suitable for investigation with different modern physical methods. The increased lifetime of the excited state and the properties of the dried samples could help in the elucidation of the properties of BR excited state, which is an important problem in the understanding the function of the protein. In addition, APB could be a good candidate as a memory storage material. The simple photocycle containing only the ground state and red-shifted intermediates makes it attractive for application as a two-state system. As it was shown by the double-flash experiments, green and red lights convert the AP to K and back, which are the basic requirement for writing and erasing data in memory, respectively.

The authors are grateful to Professor L. Keszthelyi for helpful discussion. This work was supported by National Science Research Fund of Hungary grants (OTKA) T 034788 and T 029878.

REFERENCES

Ames, J. B., and R. A. Mathies. 1990. The role of back-reactions and proton uptake during the N→O transition in bacteriorhodopsin's photocycle: a kinetic resonance Raman study. *Biochemistry.* 29: 7181–7190.

Balashov, S. P., R. Govindjee, E. S. Imasheva, S. Misra, T. G. Ebrey, Y. Feng, R. K. Crouch, and D. R. Menick. 1995. The two pK_a's of aspartate-85 and control of thermal isomerization and proton release in the arginine-82 to lysine mutant of bacteriorhodopsin. *Biochemistry.* 34:8820–8834.

Balashov, S. P., E. S. Imasheva, R. Govindjee, and T. G. Ebrey. 1996. Titration of aspartate-85 in bacteriorhodopsin: what it says about chromophore isomerization and proton release. *Biophys. J.* 70:473–481.

Balashov, S. P., N. V. Karneyeva, F. F. Litvin, and T. G. Ebrey. 1991. Bathoproducts and conformers of all-*trans* and 13-*cis* bacteriorhodopsin at 90 K. *Photochem. Photobiol.* 54:949–953.

Bamberg, E., N. A. Dencher, A. Fahr, and M. P. Heyn. 1981. Transmembranous incorporation of photoelectrically active bacteriorhodopsin in planar lipid bilayers. *Proc. Natl. Acad. Sci. U.S.A.* 78:7502–7506.

Batori-Tartsi, Z. I., K. Ludmann, and G. Váró. 1999. The effect of chemical additives on the bacteriorhodopsin photocycle. *J. Photochem. Photobiol. B.* 49:192–197.

Betancourt, F. M., and R. M. Glaeser. 2000. Chemical and physical evidence for multiple functional steps comprising the M state of the bacteriorhodopsin photocycle. *Biochim. Biophys. Acta.* 1460:106–118.

Blaurock, A. E., and W. Stoeckenius. 1971. Structure of the purple membrane. *Nature.* 233:152–155.

Butt, H. J., K. Fendler, E. Bamberg, J. Tittor, and D. Oesterhelt. 1989. Aspartic acids 96 and 85 play a central role in the function of bacteriorhodopsin as a proton pump. *EMBO J.* 8:1657–1663.

Dér, A., P. Hargittai, and J. Simon. 1985. Time-resolved photoelectric and absorption signals from oriented purple membranes immobilized in gel. *J. Biochem. Biophys. Methods.* 10:295–300.

Dér, A., L. Oroszi, A. Kulcsár, L. Zimányi, R. Tóth-Boconádi, L. Keszthelyi, W. Stoeckenius, and P. Ormos. 1999. Interpretation of the spatial charge displacements in bacteriorhodopsin in terms of structural changes during the photocycle. *Proc. Natl. Acad. Sci. U.S.A.* 96:2776–2781.

Dér, A., S. Száraz, R. Tóth-Boconádi, Z. Tokaji, L. Keszthelyi, and W. Stoeckenius. 1991. Alternative translocation of protons and halide ions by bacteriorhodopsin. *Proc. Natl. Acad. Sci. U.S.A.* 88:4751–4755.

De Groot, H. J., S. O. Smith, J. Courtin, E. Van den Berg, C. Winkel, J. Lugtenburg, R. G. Griffin, and J. Herzfeld. 1990. Solid-state ^{13}C and ^{15}N NMR study of the low pH forms of bacteriorhodopsin. *Biochemistry.* 29:6873–6883.

Dencher, N. A., H. J. Sass, and G. Büldt. 2000. Water and bacteriorhodopsin: structure, dynamics, and function. *Biochim. Biophys. Acta.* 1460:192–203.

Dioumaev, A. K., and M. S. Braiman. 1997. Two bathointermediates of the bacteriorhodopsin photocycle, distinguished by nanosecond time-resolved FTIR spectroscopy at room temperature. *J. Phys. Chem. B.* 101:1655–1662.

Drachev, L. A., A. D. Kaulen, L. V. Khitrina, and V. P. Skulachev. 1981. Fast stages of photoelectric processes in biological membranes. I. Bacteriorhodopsin. *Eur. J. Biochem.* 117:461–470.

Ebrey, T. G. 1993. Light energy transduction in bacteriorhodopsin. *In* Thermodynamics of Membranes, Receptors and Channels. M. Jackson, editor. CRC Press, New York. 353–387.

Edman, K., P. Nollert, A. Royant, H. Belrhali, E. Pebay-Peyroula, J. Hajdu, R. Neutze, and E. M. Landau. 1999. High-resolution X-ray structure of an early intermediate in the bacteriorhodopsin photocycle. *Nature.* 401: 822–826.

Fischer, U., and D. Oesterhelt. 1979. Chromophore equilibria in bacteriorhodopsin. *Biophys. J.* 28:211–230.

Ganea, C., C. Gergely, K. Ludmann, and G. Váró. 1997. The role of water in the extracellular half channel of bacteriorhodopsin. *Biophys. J.* 73: 2718–2725.

Gergely, C., C. Ganea, G. I. Groma, and G. Váró. 1993. Study of the photocycle and charge motions of the bacteriorhodopsin mutant D96N. *Biophys. J.* 65:2478–2483.

Gergely, C., C. Ganea, and G. Váró. 1994. Combined optical and photoelectric study of the photocycle of 13-*cis* bacteriorhodopsin. *Biophys. J.* 67: 855–861.

Gergely, C., L. Zimányi, and G. Váró. 1997. Bacteriorhodopsin intermediate spectra determined over a wide pH range. *J. Phys. Chem. B* 101: 9390–9395.

Golub, G., and W. Kahan. 1992. Calculating the singular values and pseudo-inverse of a matrix. *SIAM J. Num. Anal.* 2:205–224.

Groma, G. I., J. Hebling, C. Ludwig, and J. Kuhl. 1995. Charge displacement in bacteriorhodopsin during the forward and reverse bR-K phototransition. *Biophys. J.* 69:2060–2065.

Kalaidzidis, IV, and A. D. Kaulen. 1997. Cl^--dependent photovoltage responses of bacteriorhodopsin: comparison of the D85T and D85S mutants and wild-type acid purple form. *FEBS Lett.* 418:239–242.

Kelemen, L., P. Galajda, S. Száraz, and P. Ormos. 1999. Chloride ion binding to bacteriorhodopsin at low pH: an infrared spectroscopic study. *Biophys. J.* 76:1951–1958.

Keszthelyi, L., and P. Ormos. 1983. Displacement current on purple membrane fragments oriented in a suspension. *Biophys. Chem.* 18:397–405.

Konishi, T., and L. Packer. 1976. Light-dark conformational states in bacteriorhodopsin. *Biochem. Biophys. Res. Commun.* 72:1437–1442.

Korenstein, R., and B. Hess. 1977a. Hydration effects on *cis-trans* isomerization of bacteriorhodopsin. *FEBS. Lett.* 82:7–11.

Korenstein, R., and B. Hess. 1977b. Hydration effects on the photocycle of bacteriorhodopsin in thin layers of purple membrane. *Nature.* 270:184–186.

Kouyama, T., A. Nasuda-Kouyama, A. Ikegami, M. K. Mathew, and W. Stoeckenius. 1988. Bacteriorhodopsin photoreaction: identification of a long-lived intermediate N (P, R350) at high pH and its M-like photoproduct. *Biochemistry.* 27:5855–5863.

Kovács, I., and G. Váró. 1988. Charge motion in vacuum-dried bacteriorhodopsin. *J. Photochem. Photobiol. B.* 1:469–474.

Kulcsár, A., G. I. Groma, J. K. Lanyi, and G. Váró. 2000. Characterization of the proton transporting photocycle of *pharaonis* halorhodopsin. *Biophys. J.* 79:2705–2713.

Lanyi, J. K. 2000. Crystallographic studies of the conformational changes that drive directional transmembrane ion movement in bacteriorhodopsin. *Biochim. Biophys. Acta.* 1459:339–345.

Lanyi, J. K., and G. Váró. 1995. The photocycle of bacteriorhodopsin. *Isr. J. Chem.* 35:365–385.

Litvin, F. F., and S. P. Balashov. 1977. [New intermediates in the photochemical transformation of rhodopsin] in Russian. *Biofizika.* 22:1111–1114.

Logunov, S. L., M. A. El-Sayed, and J. K. Lanyi. 1996. Catalysis of the retinal subpicosecond photoisomerization process in acid purple bacteriorhodopsin and some bacteriorhodopsin mutants by chloride ions. *Biophys. J.* 71: 1545–1553.

Lozier, R. H., R. A. Bogomolni, and W. Stoeckenius. 1975. Bacteriorhodopsin: a light-driven proton pump in *Halobacterium halobium*. *Biophys. J.* 15:955–963.

Lozier, R. H., A. Xie, J. Hofrichter, and G. M. Clore. 1992. Reversible steps in the bacteriorhodopsin photocycle. *Proc. Natl. Acad. Sci. U.S.A.* 89: 3610–3614.

Ludmann, K., C. Ganea, and G. Váró. 1999. Back photoreaction from intermediate M of bacteriorhodopsin photocycle. *J. Photochem. Photobiol. B.* 49:23–28.

Ludmann, K., C. Gergely, A. Dér, and G. Váró. 1998a. Electric signals during the bacteriorhodopsin photocycle, determined over a wide pH range. *Biophys. J.* 75:3120–3126.

Ludmann, K., C. Gergely, and G. Váró. 1998b. Kinetic and thermodynamic study of the bacteriorhodopsin photocycle over a wide pH range. *Biophys. J.* 75:3110–3119.

Luecke, H., B. Schobert, H. T. Richter, J. P. Cartailler, and J. K. Lanyi. 1999a. Structural changes in bacteriorhodopsin during ion transport at 2 angstrom resolution. *Science.* 286:255–260.

Luecke, H., B. Schobert, H. T. Richter, J. P. Cartailler, and J. K. Lanyi. 1999b. Structure of bacteriorhodopsin at 1.55 Å resolution. *J. Mol. Biol.* 291: 899–911.

Maeda, A., F. L. Tomson, R. B. Gennis, H. Kandori, T. G. Ebrey, and S. P. Balashov. 2000. Relocation of internal bound water in bacteriorhodopsin during the photoreaction of M at low temperatures: an FTIR study. *Biochemistry.* 39:10154–10162.

Metz, G., F. Siebert, and M. Engelhard. 1992. Asp^{85} is the only internal aspartic acid that gets protonated in the M intermediate and the purple-to-blue transition of bacteriorhodopsin: a solid-state ^{13}C CP-MAS NMR investigation. *FEBS Lett.* 303:237–241.

Mitrovich, Q. M., K. G. Victor, and M. S. Braiman. 1995. Differences between the photocycles of halorhodopsin and the acid purple form of bacteriorhodopsin analyzed with millisecond time-resolved FTIR spectroscopy. *Biophys. Chem.* 56:121–127.

Moltke, S., and M. P. Heyn. 1995. Photovoltage kinetics of the acid-blue and acid-purple forms of bacteriorhodopsin: evidence for no net charge transfer. *Biophys. J.* 69:2066–2073.

Mowery, P. C., R. H. Lozier, Q. Chae, Y. W. Tseng, M. Taylor, and W. Stoeckenius. 1979. Effect of acid pH on the absorption spectra and photoreactions of bacteriorhodopsin. *Biochemistry.* 18:4100–4107.

Oesterhelt, D., and W. Stoeckenius. 1974. Isolation of the cell membrane of *Halobacterium halobium* and its fractionation into red and purple membrane. *Methods Enzymol.* 31:667–678.

Ormos, P., L. Reinisch, and L. Keszthelyi. 1983. Fast electric response signals in the bacteriorhodopsin photocycle. *Biochim. Biophys. Acta.* 722:471–479.

Pettei, M. J., A. P. Yudd, K. Nakanishi, R. Henselman, and W. Stoeckenius. 1977. Identification of retinal isomers isolated from bacteriorhodopsin. *Biochemistry.* 16:1955–1959.

Richter, H. T., R. Needleman, and J. K. Lanyi. 1996. Perturbed interaction between residues 85 and 204 in Tyr-185→Phe and Asp-85→Glu bacteriorhodopsins. *Biophys. J.* 71:3392–3398.

Sasaki, J., L. S. Brown, Y. S. Chon, H. Kandori, A. Maeda, R. Needleman, and J. K. Lanyi. 1995a. Conversion of bacteriorhodopsin into a chloride ion pump. *Science.* 269:73–75.

Sasaki, J., T. Yuzawa, H. Kandori, A. Maeda, and H. Hamaguchi. 1995b. Nanosecond time-resolved infrared spectroscopy distinguishes two K species in the bacteriorhodopsin photocycle. *Biophys. J.* 68:2073–2080.

Sass, H. J., G. Büldt, R. Gessenich, D. Hehn, D. Neff, R. Schlesinger, J. Berendzen, and P. Ormos. 2000. Structural alterations for proton translocation in the M state of wild-type bacteriorhodopsin. *Nature.* 406:649–653.

Scherrer, P., W. Stoeckenius, M. K. Mathew, and W. Sperling. 1987. Isomer ratio in dark-adapted bacteriorhodopsin. *In* Biophysical Studies of Retinal Proteins. T.G. Ebrey, H. Frauenfelder, B. Honig, and K. Nakanishi, editors. University of Illinois Press, Urbana-Champaign. 206–211.

Shichida, Y., S. Matuoka, Y. Hidaka, and T. Yoshizawa. 1983. Absorption spectra of intermediates of bacteriorhodopsin measured by laser photolysis at room temperatures. *Biochim. Biophys. Acta.* 723:240–246.

Smith, S. O., and R. A. Mathies. 1985. Resonance Raman spectra of the acidified and deionized forms of bacteriorhodopsin. *Biophys. J.* 47: 251–254.

Subramaniam, S. 1999. The structure of bacteriorhodopsin: an emerging consensus. *Curr. Opin. Struct. Biol.* 9:462–468.

Tokaji, Z., A. Dér, and L. Keszthelyi. 1997. N-like intermediate in the photocycle of the acid purple form of bacteriorhodopsin. *FEBS Lett.* 405: 125–127.

Trissl, H. W. 1990. Photoelectric measurements of purple membranes. *Photochem. Photobiol.* 51:793–818.

Váró, G., L. S. Brown, N. Sasaki, H. Kandori, A. Maeda, R. Needleman, and J. K. Lanyi. 1995. Light-driven chloride ion transport by halorhodopsin from *Natronobacterium pharaonis*. 1. The photochemical cycle. *Biochemistry.* 34:14490–14499.

Váró, G., and L. Eisenstein. 1987. Infrared studies of water induced conformational changes in bacteriorhodopsin. *Eur. J. Biochem.* 14:163–168.

Váró, G., and L. Keszthelyi. 1983. Photoelectric signals from dried oriented purple membranes of *Halobacterium halobium*. *Biophys. J.* 43:47–51.

Váró, G., and L. Keszthelyi. 1985. Arrhenius parameters of the bacteriorhodopsin photocycle in dried oriented samples. *Biophys. J.* 47:243–246.

Váró, G., and J. K. Lanyi. 1989. Photoreactions of bacteriorhodopsin at acid pH. *Biophys. J.* 56:1143–1151.

Váró, G., and J. K. Lanyi. 1990. Pathways of the rise and decay of the M photointermediate of bacteriorhodopsin. *Biochemistry.* 29:2241–2250.

Vonck, J. 2000. Structure of the bacteriorhodopsin mutant F219L N intermediate revealed by electron crystallography. *EMBO J.* 19:2152–2160.

Weast, R. C. Handbook of Chemistry and Physics. 1971. The Chemical Rubber Co., Cleveland, OH.

Zimányi, L., and J. K. Lanyi. 1989. Transient spectroscopy of bacterial rhodopsins with optical multichannel analyzer. 2. Effects of anions on the halorhodopsin photocycle. *Biochemistry.* 28:5172–5178.